European Journal of Pharmaceutics and Biopharmaceutics 80 (2012) 247–256

Contents lists available at SciVerse ScienceDirect

European Journal of Pharmaceutics and Biopharmaceutics

journal homepage: www.elsevier.com/locate/ejpb

Research paper

Cellular uptake mechanism and knockdown activity of siRNA-loaded biodegradable DEAPA-PVA-g-PLGA nanoparticles

Markus Benfer, Thomas Kissel *

Department of Pharmaceutics and Biopharmacy, Philipps-Universität Marburg, Marburg, Germany

ARTICLE INFO

Article history:
Received 2 June 2011
Accepted in revised form 31 October 2011
Available online 10 November 2011

Keywords:
Nanoparticles
Biodegradable polymer
siRNA delivery
Cellular uptake mechanism
Lung surfactant
Knockdown

ABSTRACT

Efficient downregulation of gene expression depends on the uptake, intracellular distribution and efficient release of siRNA from their carrier. Therefore, the cellular uptake behavior and mechanism and intracellular localization of siRNA-loaded biodegradable nanoparticles were investigated.

A biodegradable polymer, composed of poly(vinyl alcohol) (PVA) modified with diamine moieties and grafted with PLGA, abbreviated as DEAPA-PVA-g-PLGA, was used for the preparation of siRNA-loaded nanoparticles by solvent displacement. Particle sizes and morphology were determined by dynamic light scattering (DLS) and scanning electron microscopy (SEM). The dependence of particle uptake into H1299-EGFP cells (lung cancer cells expressing green fluorescent protein) on both incubation time and temperature was studied by flow cytometry. Inhibition experiments focusing on clathrin- or caveolae-mediated uptake or uptake by macropinocytosis were performed. The intracellular localization was investigated by confocal laser scanning microscopy. The GFP knockdown efficiency was determined *in vitro* to establish the potential of the nanoparticles for the downregulation of gene expression.

Nanoparticles with diameters of 120–180 nm were successfully generated. In contrast to the uptake of standard PEI-polyplexes, which increased continuously over a period of 4 h, nanoparticle uptake was complete within 2 h. A decrease in particle uptake at 4 °C (in comparison with 37 °C) suggests an active uptake process. Inhibition experiments revealed the predominance of clathrin-mediated uptake for siRNA-loaded nanoparticles. The siRNA-loaded nanoparticles could be clearly located within cells, mainly in intracellular vesicles. Particle uptake could be increased by the addition of lung surfactant to the formulation. Bioactivity in terms of successful GFP knockdown *in vitro* was demonstrated and could be further optimized by the use of surfactant-modified particles.

In conclusion, a high and rapid cellular uptake was shown for siRNA-loaded nanoparticles. Cell internalization is based on an energy-dependent and predominantly clathrin-mediated process. Particle localization in endosomes and lysosomes was demonstrated. Evidence for the efficient delivery of bioactive siRNA and specific GFP knockdown provides a solid basis for the application of DEAPA-PVA-g-PLGA-based particles for gene silencing *in vivo*.

1. Introduction

The treatment of cancer usually aims at the inhibition of cell proliferation and ideally at the induction of cell death. Gene silencing by RNA interference provides the opportunity to influence these processes by downregulation of gene expression [1]. The inhibition of protein biosynthesis, especially the synthesis of factors essential for cell growth and division, has a negative effect on tumor growth [2,3]. When gene silencing is focused on downregulation of the expression of antiapoptotic proteins (heat shock proteins), not only cell proliferation can be reduced but also cell death can be induced [4,5].

The delivery of siRNA to its cellular site of action requires the overcoming of several hurdles. One important factor is the protection of the genetic material against the rapid degradation by RNases [6]. Another major concern is the potential of siRNA to cause side effects based on immune responses [7], which can be minimized by using a suitable delivery agent. The suitability is based on characteristics like good RNA complexation, low cytotoxicity, interaction with cell membranes and degradation behavior. Various non-viral carriers based on positively charged polycations have been developed for siRNA delivery and gene silencing [8–11]. To avoid accumulation of carriers in tissues causing toxicity, recently more attention has been given to biodegradable polymers [12].

* Corresponding author. Department of Pharmaceutics and Biopharmacy, Philipps-Universität Marburg, Ketzerbach 63, 35037 Marburg, Germany. Tel.: +49 6421 2825881; fax: +49 6421 2827016.
E-mail address: kissel@staff.uni-marburg.de (T. Kissel).

0939-6411/$ - see front matter © 2011 Elsevier B.V. All rights reserved.
doi:10.1016/j.ejpb.2011.10.021

One approach combined PLGA with chitosan for the preparation of siRNA-loaded nanoparticles for GFP knockdown showing relatively low cytotoxicity [13]. Introduction of reducible disulfide bonds in poly(amido amine)s leads to biodegradable polyplexes, used for siRNA delivery [14].

Polymers of the general structure poly[vinyl-3-(dialkylamino) alkylcarbamate-co-vinyl acetate-co-vinyl alcohol]-graft-poly(D,L-lactide-co-glycolide) combine the requirements for RNA complexation and biodegradability. The polymers, abbreviated as DEAEA-, DMAPA- or DEAPA-PVA-g-PLGA, were synthesized and characterized with regard to their composition, molecular weight and degradation under physiological conditions [15]. Nanoparticles showed good complexation of DNA using P(33)-10 and P(68)-10 in comparison with a polymer with lower amine substitution [16]. Best transfection efficiency in L929 cells in comparison with other branched polyesters was achieved with P(68)-10, along with very low cytotoxicity for this polymer [16,17]. Cellular uptake behavior of plasmid DNA-loaded nanoparticles as a function of stabilizers has been studied in A549 cells [18]. A study dealing with the preparation of siRNA-containing nanoparticles and their *in vitro* knockdown efficiency was also reported [19]. A rapid degradation rate under physiological conditions, low cytotoxicity for P(68)-10 nanoparticles and high luciferase-knockdown potential with low amounts of siRNA was demonstrated. Degradation behavior, transfection properties and low cytotoxicity render this polymer an interesting and promising candidate for gene delivery.

The aim of this investigation was to characterize the cellular uptake mechanism and subsequent intracellular localization of the siRNA-carrying particles, as these factors affect the efficiency of gene knockdown. Cellular uptake of formulations based on polycations occurs usually by endocytosis, which can be mediated by clathrin, or by a clathrin-independent pathway, such as uptake by caveolae [20,21]. Assuming that the uptake of DEAPA-PVA-g-PLGA/siRNA particles is of the active type, the involvement of endocytosis in the uptake route needs to be answered.

A further point of interest was the biological activity of the nanoparticles with regard to knockdown of GFP (green fluorescent protein) expression *in vitro*. This biological activity depends not only on an efficient uptake but also on the endosomal escape of particles for efficient siRNA delivery at the site of action. A so-called proton sponge effect was proposed for polycations like poly(ethylene imine), due to its high amount of protonable amine groups [22]. Different mechanisms for the endosomal escape of DEAPA-PVA-g-PLGA particles have been considered. Possible mechanisms include endosomal rupture due to the behavior of the polymer as a proton sponge, increase in the osmotic pressure inside endosomes due to the accumulation of degradation products, fusogenic activity based on the hydrophobic polymer moieties or swelling of the polymer [16,17,19]. A successive course of different mechanisms has been discussed for the efficient down-regulation of luciferase expression *in vitro* [19]. Hence, the efficient luciferase-knockdown is based on successful endosomal escape. A further hypothesis was that the nanoparticles can also be used for efficient silencing of GFP expression. This would present the formulation as a potential tool to study gene silencing *in vivo* in GFP-expressing mice.

Additionally, the modulation of uptake behavior by the modification of nanoparticles with lung surfactant was addressed. An elevated cellular uptake has been successfully demonstrated for nanoparticles prepared in lung surfactant, compared to those prepared in water or poloxamer [18]. Based on an improved transfection of lung cancer cells [18], it was hypothesized that also knockdown efficiency can be improved by particle modification with this surfactant.

2. Materials

The polymer P(72)-8 (PVA 15000 Da modified with average 72 diethylaminopropylamine moieties and grafted with PLGA side chains of average 8 units) was synthesized by Polymaterials (Kaufbeuren, Germany) according to Wittmar et al. [23]. Hyperbranched poly(ethylene imine) 25 kDa (PEI 25 k) was a kind gift from BASF (Ludwigshafen, Germany). The anti-GFP-siRNA (5′-pACCCUGAAGUUCAUCUGCACCACcg, 3′-ACUGGGACUUCAAGUAGACGUG GUGGC), non-labeled or labeled with Alexa Fluor® 647 or Tye™-563, and the control-siRNA (5′-pCGUUAAU CGCGUAUAAU ACGCGUat, 3′-CAGCAAUUAGCGCAUAUUAUGCGCAUAp) were provided by IDT (Leuven, Belgium). Pluronic® F68 and chlorpromazine, filipin, nystatin, wortmannin, methyl-β-cyclodextrin, sucrose and glucose were purchased from Sigma Aldrich (Munich, Germany). Freeze-dried Alveofact® was provided by Lyomark (Oberhaching, Germany). Lysotracker® yellow HCK-123 for compartment staining was purchased from Invitrogen (Darmstadt, Germany). DAPI (Diamidinophenylindole) from Merck (Darmstadt, Germany) was used for cell nucleus staining. The H1299-EGFP cells were a kind gift from Dr. Camilla Foged (University of Copenhagen, Denmark). H1299-luc cells, stably expressing the enzyme luciferase, were used as before [19]. The RPMI 1640 media, fetal bovine serum and trypsin/EDTA (10×) were purchased from PAA (Cölbe, Germany). Lipofectamine™ 2000 was also purchased from Invitrogen. FACS-flow from Becton Dickinson (New York, USA) was used for flow cytometry measurements. FluorSave® (Calbiochem, San Diego, California) was used for the observation by CLSM. All media supplements and additional solvents and solutions were of analytical grade.

3. Methods

3.1. Nanoparticle preparation

Nanoparticle preparation was performed by solvent displacement according to [19]. Briefly, unlabeled or Tye™-563- or Alexa Fluor® 647-labeled siRNA was diluted with siRNA buffer (100 nM potassium acetate (KOAc), 30 mM HEPES in DEPC-water, pH adjusted to 7.5 with KOH) to a final concentration of 250 μg/ml. 50 μl of siRNA dilution was mixed with 250 μl of polymer solution and injected into 1.25 ml of 0.1% poloxamer (Pluronic® F68; w/v) under constant stirring (2 ml/min; 500 U/min). The solvent was evaporated for 1.5 h at room temperature under stirring. For larger quantities, 80 μl of siRNA dilution was mixed with 400 μl of polymer solution and injected into 2 ml of 0.1% poloxamer.

3.2. Particle size, zeta potential and morphology

Hydrodynamic particle diameters were measured using dynamic laser light scattering (DLS) with a Zetasizer (Nano ZS, Malvern Instruments, Herrenberg, Germany) as described earlier [24]. Additionally, zeta potentials were determined by laser Doppler anemometry at 25 °C, using the same instrument. Mean diameters and zeta potentials were calculated from three independent measurements.

For SEM micrographs of the nanoparticles, suspensions were deposited on silica chips and dried at room temperature. After sputter coating with platinum, samples were visualized with a JSM-7500F (JEOL, Eching, Germany). Images were taken at a working distance of 5.9 mm, with an applied electric field of 5.0 kV.

3.3. Cell culture

H1299-EGFP and H1299-luc cells were cultured in RPMI 1640 supplemented with 10% fetal bovine serum, 0.3 mg/ml glutamine, 4.5 mg/ml glucose, 2.4 mg/ml HEPES, 5 ml sodium pyruvate solution (1 mM) and 0.2 μg/ml geneticine at 37 °C and 5% CO_2. For quantitative uptake experiments, cells were seeded on 24-well plates (Nunc, Langenselbold, Germany; 3×10^4 cells/well) and incubated for 48 h at 37 °C and 5% CO_2. For confocal laser scanning microscopy (CLSM), cells were seeded in 8-chamber slides (Nunc (LabTek), Langenselbold, Germany; 1.7×10^4 cells/well) and incubated for 24 h under the same conditions. The measurement of GFP knockdown was taken with cells seeded on 24-well plates (3×10^4 cells/well) and incubated for 24 h.

3.4. Quantification of cellular uptake

Nanoparticle preparations with Alexa Fluor® 647-labeled siRNA (N/P = 8 and 15, molar ratio between the amine groups of the polymer and phosphate groups of the siRNA) were used at concentrations of 40 pmol siRNA per well. Polyplexes with PEI 25 kDa were used as a control. For preparation, PEI 25 kDa was dissolved in purified water (2 mg/ml) and appropriate volumes for N/P = 8 or 15 were diluted with 5% glucose. This polymer dilution was mixed with 8.40 μl siRNA (100 μM), which was also diluted in 5% glucose, and incubated for 15 min at room temperature before use. Free siRNA was applied as an additional control.

H1299-EGFP cells were incubated with either polyplexes or nanoparticles in RPMI 1640 for 30 min, 1 h, 2 h, 3 h or 4 h at 37 °C. Free siRNA was added for the whole incubation period of 4 h. Cells were washed twice with cold phosphate-buffered saline (PBS, pH 4.9), detached with trypsin/EDTA and finally fixed and suspended in FACS-Flow/4% paraformaldehyde (1:1). The incubations were performed in quadruplicates.

Cell-associated fluorescence was measured by flow cytometry (LSR II, Becton Dickinson, USA). For each sample, siRNA fluorescent signals of 5000 viable cells were counted for the measurement at an excitation wavelength of 632 nm. Data were analyzed with FCS Express V3.00 (DeNovo Software, Thornhill, Canada).

3.5. Intracellular uptake

Nanoparticles were prepared with Tye™-563-labeled siRNA at an N/P-ratio of 8. Polyplexes with PEI 25 kDa (N/P = 8) and pure siRNA were used as controls. The polyplexes were prepared with required amounts of polymer and siRNA as described in Section 3.4.

H1299-EGFP cells were incubated with polyplexes or nanoparticles carrying a total of 10 pmol siRNA at 37 °C for 30 min, 1 h, 2 h, 3 h or 4 h. Pure siRNA was added for 4 h. For each time point, the cells were washed twice with cold PBS (pH 4.9) and fixed with 4% paraformaldehyde in PBS (pH 7.2) for 10 min at room temperature. After washing with PBS (pH 7.4), nucleus staining was performed with DAPI solution (0.12 μg/ml) for 25 min at room temperature in the dark. Cells were washed again with PBS, the chambers were removed, and the cells were covered by the addition of FluorSave®.

Cell fluorescence was examined with a Zeiss Axiovert 100 M microscope connected to a Zeiss LSM 510 scanning device (Carl Zeiss, Jena, Germany). For excitation of DAPI fluorescence, an Enterprise laser with a wavelength of 364 nm was used. The excitation of Tye™-563 was performed with a helium–neon laser at 543 nm; an argon laser with a wavelength of 488 nm was used for GFP.

3.6. Intracellular localization

Nanoparticles were prepared by solvent displacement with Tye™-563-labeled anti-GFP-siRNA (N/P = 8). Lysotracker® was diluted in serum-free media to a series of 50–100 nM. These dilutions were added to H1299-luc cells seeded on chamber slides. The nanoparticles were added in an amount equal to 10 pmol siRNA, and cells were incubated for 30 min, 1 h or 2 h at 37 °C. After each incubation time point, the cells were washed with cold PBS (pH 4.9) and fixed with 4% paraformaldehyde, and the cell nucleus was stained with DAPI in the dark. Cells were mounted in FluorSave® for the observation by confocal laser scanning microscopy (CLSM). Lysotracker and the labeled siRNA were excited at 458 and 543 nm, respectively.

3.7. Route of cellular uptake

To investigate whether the intracellular uptake was energy-dependent, cells were incubated with the particles, carrying Alexa Fluor® 647-labeled siRNA, at 4 °C and 37 °C. H1299-EGFP cells were incubated with siRNA-loaded particles or polyplexes at the respective temperatures for 30 min. Afterward, cells were treated as described earlier for the uptake quantification.

Uptake in the presence of different uptake inhibitors was investigated on H1299-EGFP cells, which were incubated with dilutions of chlorpromazine (10 μg/ml), sucrose (0.45 M), filipin (5 μg/ml), nystatin (10 μg/ml), wortmannin (12.8 ng/ml) or methyl-β-cyclodextrin (methyl-β-CD; 6.6 mg/ml) in serum-free media for 30 min at 37 °C. After that, either particles or polyplexes (N/P = 8) were added and incubated for 3 h at 37 °C, before cells were treated for the measurement by flow cytometry as described before.

Polyplexes and nanoparticles were applied in amounts corresponding to 40 pmol siRNA, and cells were treated in quadruplicates. Cell-associated fluorescence was measured by flow cytometry using the Becton Dickinson LSR II. For each sample, 10^4 viable cells were measured. Fluorescence was excited at 632 nm.

3.8. Cellular uptake of nanoparticles prepared in lung surfactant

Nanoparticles were prepared with Alexa Fluor® 647-labeled siRNA at N/P = 8. Pure water, 0.1% poloxamer (w/v) or three different concentrated lung surfactant suspensions (Alveofact®) were chosen as a aqueous dispersion medium. H1299-EGFP cells were incubated with the particle suspensions at 37 °C for 4 h ($n = 4$) and treated for the measurement by flow cytometry as described in Section 3.4. The measurement of 10^4 viable cells per sample was taken with a BD LSR II, and fluorescence was excited at 632 nm.

3.9. GFP knockdown in vitro

Nanoparticles with N/P = 8 and 15, which were prepared in pure water, 0.1% poloxamer or 0.015% lung surfactant, were used for the GFP knockdown in H1299-EGFP cells. Lipoplexes based on lipofectamine were prepared according to the manufacturer manual. Preparation of PEI-polyplexes was performed as described in Section 3.4 with required amounts of polymer and siRNA. These two formulations were used as controls. Cells were incubated with amounts of the formulations equating to 40 pmol siRNA in serum-free RPMI 1640 at 37 °C for 4 h. The supernatant was removed, and the cells were incubated for further 44 h in fresh culture medium in quadruplicates for each sample.

After completion of the incubation time, cells were washed and treated for flow cytometry measurements as described earlier. The

GFP fluorescence was measured using a BD FACScan. GFP fluorescence was excited at 488 nm.

4. Results and discussion

4.1. Particle size, zeta potential and morphology

The polymer used for this study was DEAPA-PVA-g-PLGA with an average of 72 amine moieties (DEAPA) attached to the PVA backbone (poly(vinyl alcohol)) and grafting with PLGA chains of average 8 units (P(72)-8). The physical properties of this polymer were M_w = 270.59 kDa, M_n = 192.98 kDa, PDI = 1.40 and T_g = 6.67 °C as determined by gel permeation chromatography (GPC) and differential scanning calorimetry (DSC) according to previously published methods [23].

The size measurements by DLS revealed mean nanoparticle diameters of 120–180 nm depending on the N/P-ratio (Fig. 1a). A minor particle population with sizes below 50 nm was visible in all cases. This bimodal distribution resulted in a polydispersity index in the range of 0.26–0.56. The particle diameter is of importance, as it influences the cellular uptake behavior and the clearance from blood stream by the mononuclear phagocytic system (MPS) *in vivo* [25,26].

Increasing the N/P-ratio causes an increase in positive charge resulting in a better complexation and higher condensation of the siRNA and smaller particles [27]. Concurrently, a high N/P-ratio is linked to a high polymer concentration, thus leading to increasing particle sizes [28]. These opposite phenomena are represented by the consistent particle sizes for N/P ⩾ 6. Additionally, smaller particle sizes could be achieved in comparison with earlier results [19]. This can possibly be attributed to the slightly differing composition of the polymer in comparison with P(68)-10 with regard to DEAPA-modification and the PLGA-chain length. Due to the positive charge of the DEAPA moiety, the zeta potential was clearly positive for all cases (Fig. 1a), which is an important requirement for a good interaction of the particles with the cell membrane.

Besides particle size, the shape is an important parameter for the uptake into cells and tissues, meaning that spherical particles can be taken up more easily than non-spherical ones [25]. For the latter, the orientation of the particles to the cell membrane is decisive for the uptake efficiency. In the present case, particle preparation by solvent displacement resulted in spherical structures of homogeneous shape (Fig. 1b).

Due to the determined sizes, surface charges and the shape, a good interaction of the particles with the cell membrane and high intracellular uptake was assumed.

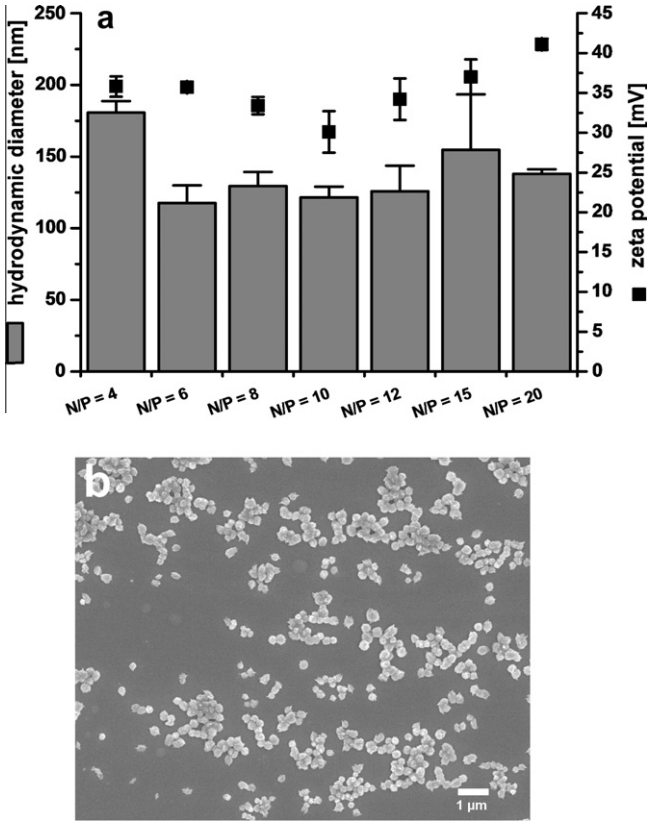

Fig. 1. Nanoparticle sizes, zeta potentials and morphology; (a) mean particle diameters determined by DLS, zeta potentials determined by laser Doppler anemometry; measurements were taken in 0.1% poloxamer (w/v) with three measurements for each sample; values are presented as mean ± sd; (b) SEM image of nanoparticles, N/P = 15; scalebar = 1 µm.

4.2. Cellular uptake and localization

Based on previously published data [19], an N/P-ratio of 8 was chosen for the uptake studies, because it is known to have a high knockdown efficiency with no unspecific effects. Nanoparticles at N/P = 15 were chosen for comparison due to their properties regarding good knockdown efficiency despite a low amount of siRNA. A standard cationic gene carrier namely PEI 25 k was used for polyplexes as a control because of its strong DNA/RNA complexation.

For the measurement of the intracellular amount of particles by flow cytometry, the fluorescence intensity of untreated cells (blanks) was set between 200 and 300. Washing after cell incubation with cold PBS (pH 4.9) was performed to guarantee the removal of particles located on the cell surface and only measuring of fluorescence coming from internalized particles.

As early as 30 min after treatment, high fluorescence values could be measured within the cells, implying a high uptake during this short incubation period (Fig. 2). A pronounced increase in uptake could be observed for PEI-polyplexes after 4 h, while the nanoparticles showed only a slight increase in cellular uptake after time point 1 h. The majority of nanoparticle uptake happened during the first hour. No significant difference could be determined for the particle-associated fluorescence between 2 h and 4 h of incubation (one-way ANOVA, $p \leqslant 0.05$), indicating that the uptake is almost complete within 2 h. Similar results for the uptake of complexes based on modified cyclodextrin prove the rapid cellular uptake of cationic nanoparticles [29].

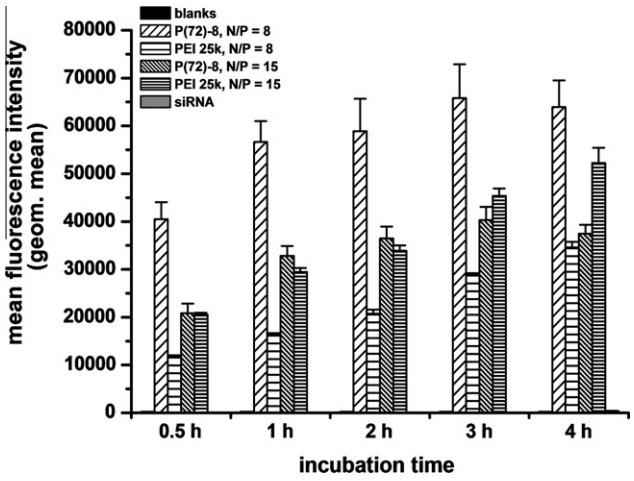

Fig. 2. Cellular uptake of siRNA-loaded nanoparticles and PEI-polyplexes, as determined by flow cytometry, siRNA labeled with Alexa Fluor® 647, excitation wavelength 632 nm; values are presented as mean ± sd, n = 4.

In comparison, the uptake of PEI-polyplexes increased continuously and reached the uptake level of nanoparticles after 4 h (Fig. 2). The uptake profiles for N/P = 15 are in agreement with those published by Nguyen et al. [18]. In contrast, the uptake of the particles with N/P = 8 was remarkably higher than the uptake of equally loaded polyplexes. The lower uptake of nanoparticles with N/P = 15 might be attributed to a higher toxicity. In contrast to PEI-polyplexes, a much higher polymer concentration is used for the preparation of nanoparticles with the same N/P-ratio. Due to the high amine density of PEI, a much lower amount of polymer

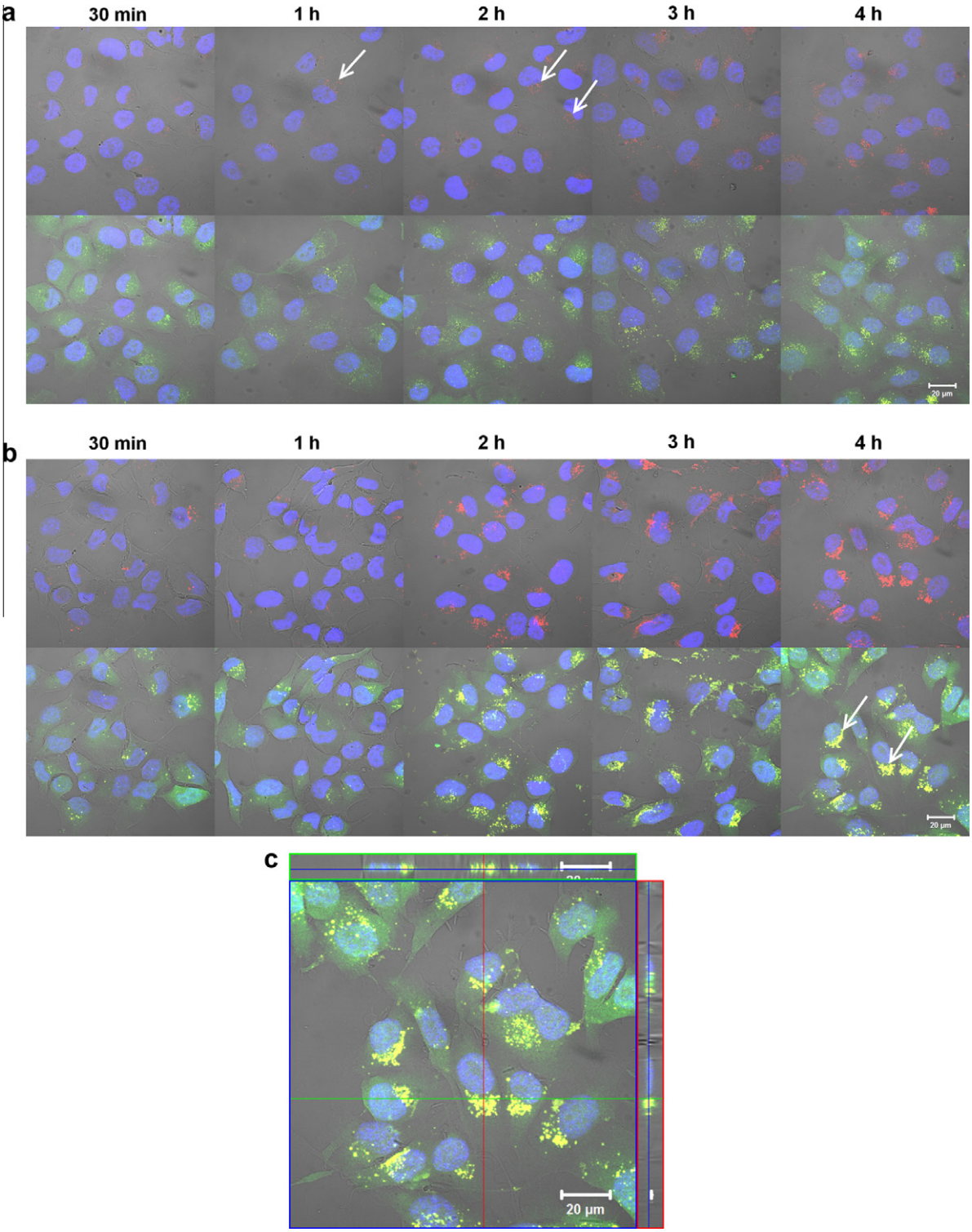

Fig. 3. Cellular uptake and intracellular localization of siRNA-loaded nanoparticles and PEI-polyplexes, as determined by CLSM; (a) cells were incubated with PEI-polyplexes for indicated times (upper row: siRNA fluorescence, lower row: GFP- and siRNA fluorescence), (b) cells were incubated with P(72)-8 nanoparticles for indicated times (upper row: siRNA fluorescence, lower row: GFP- and siRNA fluorescence); (c) series of z-stack of cells incubated with P(72)-8 nanoparticles for 4 h; excitation wavelength: DAPI 364 nm, GFP 488 nm, siRNA (Tye™-563) 543 nm; scale bar = 20 µm. (For interpretation of the references to color in this figure legend, the reader is referred to the web version of this article.)

is necessary to generate polyplexes with a certain N/P-ratio. This PEI amount is in the range of low cytotoxicity [19].

The intracellular presence of nanoparticles was observed by confocal laser scanning microscopy (CLSM). For each image, a comparison of pure siRNA fluorescence (Tye™-563) and the combination of both fluorescence signals (Tye™-563 + GFP) are presented.

For the PEI-polyplexes, cellular fluorescence increased continuously over time, which implies a continuous increase in polyplex uptake (Fig. 3a). The lower uptake in comparison with nanoparticles, as already observed by flow cytometry, could be confirmed (see arrows). One reason could be the slower sedimentation of polyplexes onto the cells due to their lower mass density, in comparison with the nanoparticles. Another point is the polyplex structure. PEI 25 k demonstrates strong binding, but incomplete incorporation of siRNA, leading to patchy self-assembled complexes [30]. The consequences are lower zeta potentials in comparison with the particles (data not shown) and a higher tendency for aggregation, both of which cause a lower cellular uptake. As the polyplex aggregation tendency matches the higher toxicity of the nanoparticles at N/P = 15, the extent of the uptake is comparable.

An increase in fluorescence intensity with longer incubation time was also observed for the nanoparticles, whereas it hardly changed after 2 h (Fig. 3b). This also confirms the flow cytometry results. Another remarkable observation was the punctual intracellular concentration of particles with increasing incubation time, indicating localization in certain compartments. Endocytosis is the main mechanism for cellular uptake of non-viral vectors and leads to entrapment inside intracellular vesicles, which can be characterized as endosomes or lysosomes [21,31]. Additionally, extension of spot size and coalescence of spots was visible with longer incubation (Fig. 3b, arrows). This might be indicative of vesicle fusion and release of the particles or siRNA after rupture of the compartments. Release of PEI-based complexes from endosomes/lysosomes has been demonstrated by confocal microscopy by Merdan et al. [32]. The observation of fluorescence spot extension over time was seen as a possible indication for increase in vesicles or fusion with other vesicles. The burst of vesicles and release of complexes were concluded from fluorescence extension and coalescence of the spots and subsequent distribution of fluorescence throughout the cells.

No siRNA-associated fluorescence was observed for untreated cells (blanks) or those treated with pure siRNA (Supplementary data, Fig. S1). CLSM images of the samples show representative sections from a series of recorded z-stacks, to confirm that the fluorescence is located inside the cells (see also Fig. 3c). The co-localization of GFP fluorescence, which was distributed all over the cytosol, and particle fluorescence indicated that nanoparticles were successfully taken up into the cells.

The observation of nanoparticle localization in intracellular compartments was further analyzed with regard to possible particle entrapment inside endosomes or lysosomes. The intracellular localization of nanoparticles is of great importance, as it influences the delivery of the active ingredient to the site of action. As the carrier composition controls the mechanism of cellular uptake, it greatly affects the localization inside the cell. A mainly clathrin-mediated uptake and a resulting entrapment in lysosomes have been demonstrated for doxorubicin-conjugated PAMAM–dendrimers [33]. Contreras et al. have shown that polylactide-based nanoparticles are also taken up by energy-dependent endocytosis and located in perinuclear compartments, but not inside lysosomes [34]. As shown by Douglas et al., the endocytosis pathway can depend on the cell type and can therefore lead to entrapment of particles in different compartments. The uptake of alginate-chitosan nanoparticles into 293T cells involves trafficking to late endosomes or lysosomes followed by escape of the particles into the cytosol. In contrast, the uptake of such particles into CHO cells was concluded to lead to entrapment inside caveosomes, which prevents transfection [35].

To determine the intracellular localization of the siRNA-loaded particles in H1299 cells, staining with the Lysotracker® was performed during particle uptake. As mentioned by the manufacturer, the Lysotracker® recognizes acidic organelles like lysosomes. A co-localization of the red siRNA fluorescence and the green lysotracker fluorescence was visible after cell treatment with both components (Fig. 4a–c). This observation demonstrates a particle localization inside acidic compartments. Since the acidification of endosomal organelles takes place at the level of early endosomes [21], a differentiation between stained late endosomes and lysosomes cannot be made. Hence, it can be concluded that the nanoparticles are localized both inside endosomes and lysosomes from which they seem to escape. This would be in agreement with the indications for compartment fusion and rupture over the time after uptake (Fig. 3b). Besides the considered escape mechanisms, endosomal release could also be attributed to the PLGA side chains to some extent. Rapid endosomal escape has been observed for PLGA nanoparticles, which was explained by a cationization of the polymer in the acidic environment [36]. This might enhance the release from endosomes in the case of the DEAPA-PVA-g-PLGA nanoparticles. Since microscopy does not allow for quantitative analysis, a quantification of the localization inside lysosomes or endosomes cannot be made. Therefore, a fractionation of subcellular organelles after incubation with particles or an incubation in the presence of

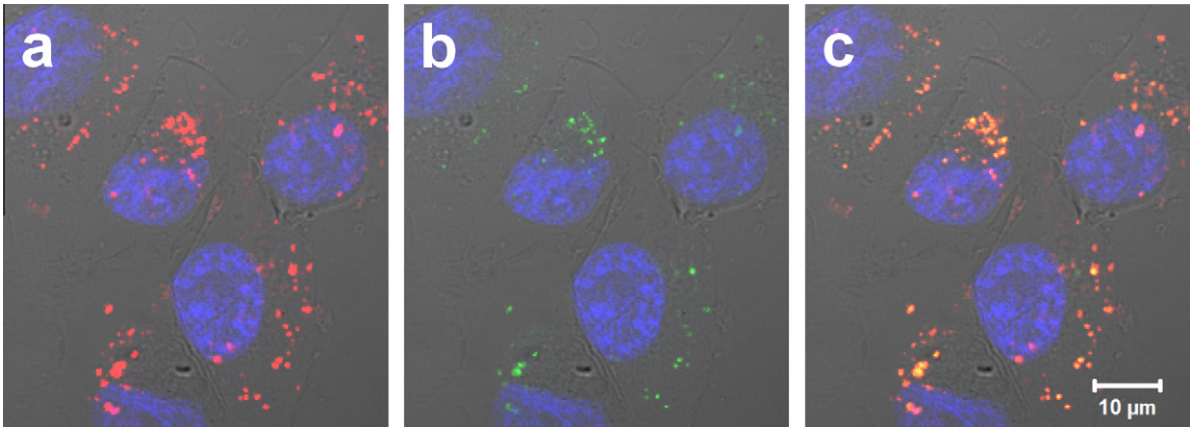

Fig. 4. Intracellular localization of siRNA-loaded nanoparticles, as determined by CLSM; (a–c) cells were incubated with nanoparticles (1 h) in the presence of lysotracker® yellow (100 nM) ((a) siRNA fluorescence, (b) lysotracker, (c) siRNA and lysotracker); excitation wavelength: DAPI 364 nm, siRNA (Tye™-563) 543 nm, lysotracker 458 nm. (For interpretation of the references to color in this figure legend, the reader is referred to the web version of this article.)

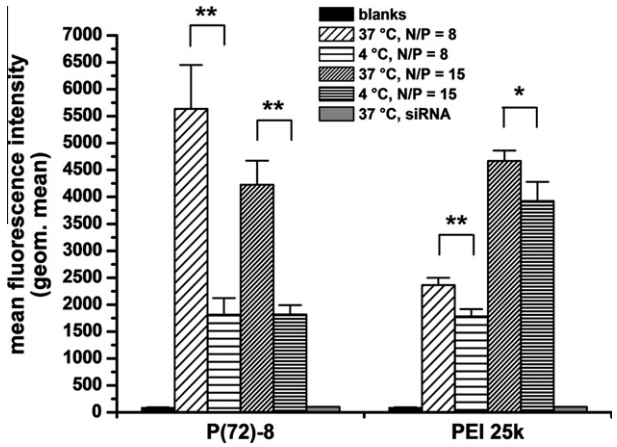

Fig. 5. Comparison of nanoparticle and polyplex uptake at 37 °C and 4 °C, as determined by flow cytometry, siRNA labeled with Alexa Fluor® 647, excitation wavelength 632 nm; values are presented as mean ± sd, $n = 4$; $^{*}p \leqslant 0.05$, $^{**}p \leqslant 0.01$.

bafilomycin that prevents the acidification of endosomes would be helpful to determine particle localization in a quantitative way [37].

4.3. Route of cellular uptake

A high and rapid cellular uptake and entrapment inside endosomes and lysosomes has been demonstrated for the nanoparticle formulation. The next question to be answered was which kind of mechanism these results can be attributed to.

To confirm that nanoparticle uptake into H1299-EGFP is an active, energy-dependent one, the cellular uptake was analyzed under two different temperature conditions. The incubation at 37 °C, providing the condition for normal cell metabolism, was compared to incubation at 4 °C. A significant decrease in nanoparticle and polyplex uptake was determined after incubation at 4 °C due to the downregulated cell metabolism (Fig. 5, *t*-test, $p \leqslant 0.05$ and $p \leqslant 0.01$). This observation indicates an active uptake mechanism for the particles. The lower temperature had a lower effect on the uptake of the polyplexes, which suggests an additional non-specific uptake for these formulations.

In order to obtain information about the route of particle internalization, the cellular uptake was analyzed in the presence of different uptake inhibitors. As gene silencing takes place at the mRNA stage in the cytosol [1], fate of the particles inside the cells and the intracellular localization have to ensure the availability of siRNA in this compartment. A localization inside endosomes, the release from these compartments or possible transfer into lysosomes followed by degradation, or an uptake mechanism independent from endosomes determines the efficiency of siRNA delivery into the cytosol [21].

Several substances are known for the inhibition of different uptake routes into cells. Chlorpromazine and sucrose have been used for the inhibition of clathrin-mediated endocytosis [38,39]. Filipin and nystatin are known to interact with cholesterol and have an influence on caveolae-mediated uptake [40,41]. Wortmannin was chosen in order to study inhibition of macropinocytosis [42]. Methyl-β-cyclodextrin is also known to interact with cholesterol and to extract it from the membrane and therefore, has an effect on clathrin- and caveolae-mediated uptake [43,44]. Besides the fact that the uptake mechanism depends on the carrier composition [21], a role of cell type has to be considered. For alginate-chitosan complexes, Douglas et al. have revealed a predominant clathrin-mediated uptake in 293T cells, a caveolin-mediated one in CHO cells and a combination of both mechanisms in COS-7 cells [35]. For poly(ethylene imine) as a standard transfection agent, two different uptake routes, a clathrin- and a caveolae-dependent one, are known. A dependence on the cell type has also been worked out in this case [45].

To determine the uptake route in H1299-EGFP cells, the fluorescence of cells treated with the respective formulations without any inhibitor was set to 100%. Cell-associated fluorescence was significantly decreased after incubation in the presence of chlorpromazine, methyl-β-cyclodextrin and sucrose, demonstrating an inhibition of particle uptake (Fig. 6, *t*-test, $p \leqslant 0.01$). These data indicate that clathrin-mediated uptake was inhibited by disturbance of the formation of clathrin-coated pits. An influence on caveolae formation can be ruled out, due to the absence of negative effects from filipin and nystatin. The small effect of wortmannin on

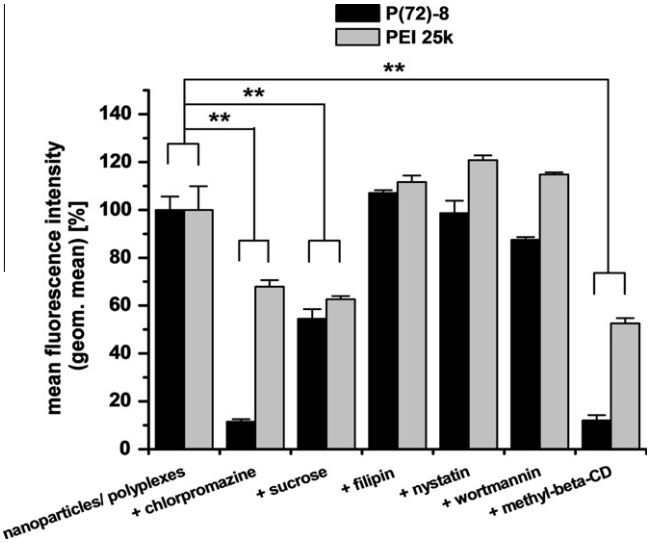

Fig. 6. Cellular uptake of nanoparticles and polyplexes in the presence of uptake inhibitors, as determined by flow cytometry, siRNA labeled with Alexa Fluor® 647, excitation wavelength 632 nm, mean fluorescence intensity of cells incubated only with nanoparticles or polyplexes was set as 100%; values are presented as mean ± sd, $n = 4$; $^{**}p \leqslant 0.01$.

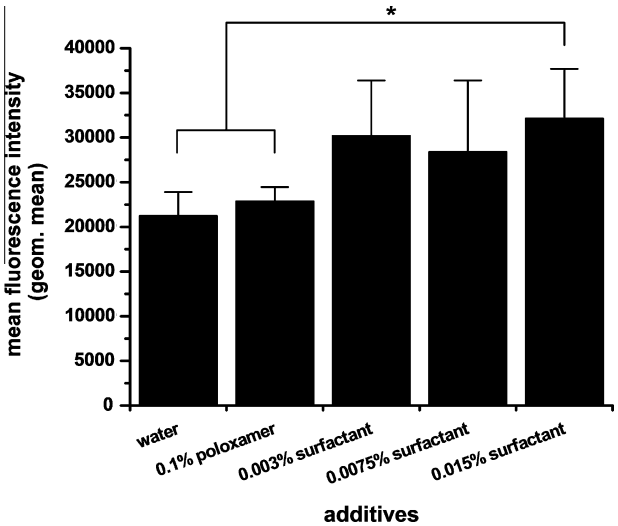

Fig. 7. Cellular uptake of nanoparticles prepared in aqueous media with different additive concentrations (w/v), as determined by flow cytometry, siRNA labeled with Alexa Fluor® 647, excitation wavelength 632 nm; values are presented as means ± sd, $n = 4$; $^{*}p \leqslant 0.05$.

nanoparticle uptake showed that macropinocytosis is presumably involved to a lesser extent.

The effect of the inhibitors was remarkably lower for the polyplex uptake, confirming the assumption of a non-specific cellular uptake mechanism for this formulation beside the clathrin-mediated one. Since PEI 25 k is known to cause destabilization of plasma membranes [46], the so-caused high permeability possibly leads to an unregulated polyplex influx into the cells. A passive polyplex uptake can also be assumed for the determination of cellular uptake at 4 °C.

The particle trafficking inside endosomes and lysosomes is confirmed by the determination of the predominantly clathrin-mediated uptake, as this mechanism leads to entrapment inside those compartments.

4.4. Cellular uptake of nanoparticles prepared in lung surfactant

A further point of interest was the modulation of particle uptake in terms of a high gene silencing efficiency. The cellular uptake of DEAPA-PVA-g-PLGA-based nanoparticles can be elevated by modification with lung surfactant [18], which consists mainly of dipalmitoylphosphatidylcholine and other phospholipids. Under the assumption that this effect is transferable to the delivery of siRNA, nanoparticles were prepared in suspensions of lung surfactant. Different concentrations were used to evaluate the most appropriate condition for uptake improvement. The uptake of these formulations was compared to that of particles prepared in pure water or poloxamer solution.

An increased cellular uptake was determined for DEAPA-PVA-g-PLGA nanoparticles prepared in surfactant (Fig. 7). The uptake was significantly higher for 0.015% surfactant as preparation medium in comparison with poloxamer or pure water (t-test, $p \leqslant 0.05$). Based on the possible particle formation [18], this phenomenon can be attributed to the formation of a lipid shell around the particles and thus to an enhanced particle interaction with the cell membrane. Hydrophobic interactions or a membrane fusion process, which is described for phospholipid vesicles [47], especially for those having a net negative surface charge [48], possibly cause this enhancement. Since the main component phosphatidylcholine comprises a zwitterionic headgroup, electrostatic interaction by the surfactant with the cell membrane supposedly plays a minor role.

Additionally, the stability of these modified formulations was analyzed with regard to the long-term storage life and applicability, analogous to formulations in water or poloxamer. Measurement of particle size and count rate by DLS over a period of 6 h showed no particle aggregation or sedimentation for formulations in water or poloxamer solution (Supplementary data, Fig. S2a and b). In the case of surfactant as the preparation medium, fluctuating particle sizes after 2 h demonstrated probable aggregation and redistribution processes based on electrostatic interaction (Fig. S2c). However, in this case, no sedimentation could be determined.

In comparison with nanoparticles prepared in pure water or poloxamer solution, which show a high stability, the long-term stability with surfactant as the additive is limited, but remains sufficient to allow for the use of the particles for *in vitro* applications.

4.5. GFP knockdown in vitro

After characterizing the delivery of siRNA inside H1299-EGFP cells, the potential of the nanoparticles for gene silencing needed to be confirmed. As the nanoparticles are intended as a tool to enforce downregulation of gene expression *in vivo*, their GFP-knockdown potential was tested *in vitro*.

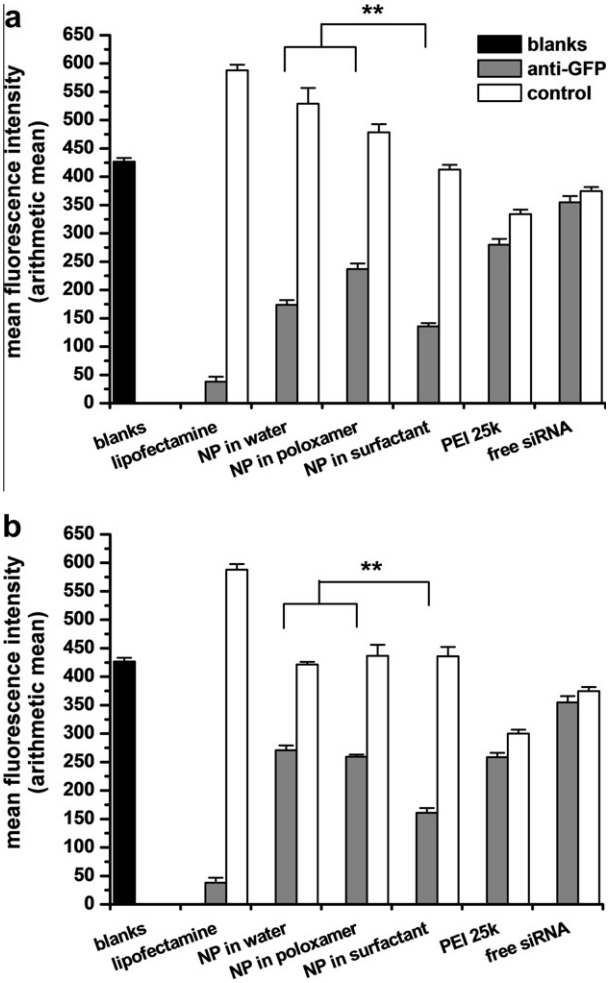

Fig. 8. Knockdown of GFP expression, as determined by flow cytometry, excitation wavelength 488 nm; (a) N/P = 8, (b) N/P = 15. Values are presented as mean ± sd, $n = 4$; $^{**}p \leqslant 0.01$, NP = nanoparticles.

Based on previous data concerning transfection efficiency [18], GFP knockdown of three different formulations was compared. A surfactant concentration of 0.015% was chosen for particle preparation due to the best results for improved nanoparticle uptake. Fig. 8 shows the mean GFP fluorescence intensity after incubation of cells with the different formulations. Results are given for two different N/P-ratios. A significant downregulation of GFP expression was determined for all formulations, namely lipofectamine, nanoparticles and polyplexes (Fig. 8, t-test, $p \leqslant 0.01$). The knockdown efficiency was significantly higher for nanoparticles prepared in lung surfactant in comparison with those prepared in pure water or poloxamer solution (t-test, $p \leqslant 0.01$). Compared with untreated cells, an efficiency of almost 70% was achieved with this formulation, meaning an improvement of about 50% in relation to the particles in poloxamer (N/P = 8). The results are in good agreement with those which have been worked out by Nguyen et al. for transfection showing a significant increase in luciferase expression by nanoparticles prepared in lung surfactant [18]. GFP knockdown could also be achieved by PEI-polyplexes, but this is a result of non-specific effects to some extent. This minor effective knockdown is in agreement with the luciferase-knockdown potential of polyplexes in comparison with the nanoparticles [19].

The data confirm an efficient delivery of bioactive siRNA into the cytosol after cellular uptake. A successful release of nanoparticles or siRNA from endosomes or lysosomes can be concluded. Possible reasons for the improved knockdown efficiency of

nanoparticles prepared in lung surfactant are the facilitated cellular uptake and an improved endosomal escape. The first effect is based on membrane fusion [47] due to the lipid particle shell, and the latter occurs due to additional destabilization of the endosomal membrane [49]. A downregulated gene expression due to unspecific toxic effects can be excluded for this formulation, since no effect was obvious when unspecific siRNA was used as a control (Fig. 8). As the gene silencing potential could not be increased by elevating the N/P-ratio, the nanoparticles can be seen as more effective at lower N/P-ratios in contrast to PEI 25 k.

PEI-polyplexes are less efficient due to their stronger aggregation tendency [30] and lower uptake. Additionally, the stronger siRNA complexation leads to lower release levels of siRNA in comparison with the particles [19]. Increase in the N/P-ratio leads not only to slightly elevated knockdown but also to an unspecific downregulation due to intracellular toxic effect based on the non-degradable polymer.

5. Conclusion

Biodegradable DEAPA-PVA-g-PLGA polyesters are suitable for the preparation of spherically shaped, nanosized particles for the delivery of siRNA. The nanoparticles are taken up rapidly into cells within 2 h and are located in compartments, which were identified as endosomes or lysosomes. The uptake mechanism is energy-dependent and based on a clathrin-mediated uptake route, confirming the particle trafficking inside endosomes.

Particle modification with lung surfactant results in a formulation with characteristics for enhanced cellular uptake. Concerning the *in vitro* potential, the nanoparticles can be used for specific GFP knockdown, confirming a successful endosomal escape. Addition of lung surfactant leads to an improvement of knockdown efficiency by approximately 50% compared to particles in poloxamer solution.

In summary, the results confirm that DEAPA-PVA-g-PLGA-based nanoparticles are efficient carriers for siRNA delivery *in vitro*. With regard to the application *in vivo,* the question of particle behavior in the presence of serum has to be answered, when opting for an intravenous application of the nanoparticles. Nevertheless, the data given here present the promising basis for a local application *in vivo*, for example, in the lung.

Acknowledgements

The authors want to thank Michael Hellwig from the working group of Dr. Schaper for taking the SEM images. Additionally, we want to thank Dr. Juliane Nguyen for providing the synthesis protocol and Thomas Endres for performing the GPC measurement. We are grateful for the support by the European Commission (Sixth Framework Programme, Integrated Project Meditrans, Targeted Delivery of Nanomedicine).

Appendix A. Supplementary material

Supplementary data associated with this article can be found, in the online version, at doi:10.1016/j.ejpb.2011.10.021.

References

[1] C. Huang, M. Li, C. Chen, Q. Yao, Small interfering RNA therapy in cancer: mechanism potential targets and clinical applications, Expert Opin. Ther. Targets 12 (2008) 637–645.
[2] X. Zhang, Y.L. Ge, R.H. Tian, The knockdown of c-myc expression by RNAi inhibits cell proliferation in human colon cancer HT-29 cells in vitro and in vivo, Cell. Mol. Biol. Lett. 14 (2009) 305–318.
[3] S. Höbel, I. Koburger, M. John, F. Czubayko, P. Hadwiger, H.P. Vornlocher, A. Aigner, Polyethylenimine/small interfering RNA-mediated knockdown of vascular endothelial growth factor in vivo exerts anti-tumor effects synergistically with Bevacizumab, J. Gene Med. 12 (2010) 287–300.
[4] X.X. Liu, P. Rocchi, F.Q. Qu, S.Q. Zheng, Z.C. Liang, M. Gleave, J. Iovanna, L. Peng, PAMAM dendrimers mediate siRNA delivery to target Hsp27 and produce potent antiproliferative effects on prostate cancer cells, ChemMedChem 4 (2009) 1302–1310.
[5] Q. Zhu, Y.M. Xu, L.F. Wang, Y. Zhang, F. Wang, J. Zhao, L.T. Jia, W.G. Zhang, A.G. Yang, Heat shock protein 70 silencing enhances apoptosis inducing factor-mediated cell death in hepatocellular carcinoma HepG2 cells, Cancer Biol. Ther. 8 (2009) 792–798.
[6] S. David, B. Pitard, J.P. Benoit, C. Passirani, Non-viral nanosystems for systemic siRNA delivery, Pharmacol. Res. 62 (2010) 100–114.
[7] M. Sioud, RNA interference and innate immunity, Adv. Drug Deliv. Rev. 59 (2007) 153–163.
[8] A. Tamura, Y. Nagasaki, Smart siRNA delivery systems based on polymeric nanoassemblies and nanoparticles, Nanomedicine (London) 5 (2010) 1089–1102.
[9] D. Jere, H.L. Jiang, Y.K. Kim, R. Arote, Y.J. Choi, C.H. Yun, M.H. Cho, C.S. Cho, Chitosan-graft-polyethylenimine for Akt1 siRNA delivery to lung cancer cells, Int. J. Pharm. 378 (2009) 194–200.
[10] A.K. Varkouhi, R.J. Verheul, R.M. Schiffelers, T. Lammers, G. Storm, W.E. Hennink, Gene silencing activity of siRNA polyplexes based on thiolated N,N,N-trimethylated chitosan, Bioconjug. Chem. 21 (2010) 2339–2346.
[11] P. Ofek, W. Fischer, M. Calderon, R. Haag, R. Satchi-Fainaro, In vivo delivery of small interfering RNA to tumors and their vasculature by novel dendritic nanocarriers, Faseb J. 24 (2010) 3122–3134.
[12] J. Luten, C.F. van Nostrum, S.C. De Smedt, W.E. Hennink, Biodegradable polymers as non-viral carriers for plasmid DNA delivery, J. Control. Release 126 (2008) 97–110.
[13] X. Yuan, B.A. Shah, N.K. Kotadia, J. Li, H. Gu, Z. Wu, The development and mechanism studies of cationic chitosan-modified biodegradable PLGA nanoparticles for efficient siRNA drug delivery, Pharm. Res. 27 (2010) 1285–1295.
[14] P. Vader, L.J. van der Aa, J.F.J. Engbersen, G. Storm, R.M. Schiffelers, Disulfide-based poly(amino amine)s for siRNA delivery: effects of structure on siRNA complexation cellular uptake gene silencing and toxicity, Pharm. Res. 28 (2011) 1013–1022.
[15] M. Wittmar, Charge modified, comb-like graft-polyesters for drug delivery and DNA vaccination: synthesis and characterization of poly(vinyl dialkylaminoalkylcarbamate-co-vinyl acetate-co-vinyl alcohol)-graft-poly(D,L-lactide-co-glycolide)s, PhD Thesis, Philipps University, Marburg, 2004.
[16] C.G. Oster, M. Wittmar, U. Bakowsky, T. Kissel, DNA nano-carriers from biodegradable cationic branched polyesters are formed by a modified solvent displacement method, J. Control. Release 111 (2006) 371–381.
[17] C.G. Oster, M. Wittmar, F. Unger, L. Barbu-Tudoran, A.K. Schaper, T. Kissel, Design of amine-modified graft polyesters for effective gene delivery using DNA-loaded nanoparticles, Pharm. Res. 21 (2004) 927–931.
[18] J. Nguyen, R. Reul, T. Betz, E. Dayyoub, T. Schmehl, T. Gessler, U. Bakowsky, W. Seeger, T. Kissel, Nanocomposites of lung surfactant and biodegradable cationic nanoparticles improve transfection efficiency to lung cells, J. Control. Release 140 (2009) 47–54.
[19] J. Nguyen, T.W. Steele, O. Merkel, R. Reul, T. Kissel, Fast degrading polyesters as siRNA nano-carriers for pulmonary gene therapy, J. Control. Release 132 (2008) 243–251.
[20] C. Pichon, L. Billiet, P. Midoux, Chemical vectors for gene delivery: uptake and intracellular trafficking, Curr. Opin. Biotechnol. 21 (2010) 640–645.
[21] I.A. Khalil, K. Kogure, H. Akita, H. Harashima, Uptake pathways and subsequent intracellular trafficking in nonviral gene delivery, Pharmacol. Rev. 58 (2006) 32–45.
[22] O. Boussif, F. Lezoualc'h, M.A. Zanta, M.D. Mergny, D. Scherman, B. Demeneix, J.P. Behr, A versatile vector for gene and oligonucleotide transfer into cells in culture and in vivo: polyethylenimine, Proc. Natl. Acad. Sci. USA 92 (1995) 7297–7301.
[23] M. Wittmar, F. Unger, T. Kissel, Biodegradable brushlike branched polyesters containing a charge-modified poly(vinyl alcohol) backbone as a platform for drug delivery systems: synthesis and characterization, Macromolecules 39 (2006) 1417–1424.
[24] T. Merdan, K. Kunath, H. Petersen, U. Bakowsky, K.H. Voigt, J. Kopecek, T. Kissel, PEGylation of poly(ethylene imine) affects stability of complexes with plasmid DNA under in vivo conditions in a dose-dependent manner after intravenous injection into mice, Bioconjug. Chem. 16 (2005) 785–792.
[25] M. Caldorera-Moore, N. Guimard, L. Shi, K. Roy, Designer nanoparticles: incorporating size shape and triggered release into nanoscale drug carriers, Expert Opin. Drug Deliv. 7 (2010) 479–495.
[26] D.E. Owens 3rd, N.A. Peppas, Opsonization biodistribution and pharmacokinetics of polymeric nanoparticles, Int. J. Pharm. 307 (2006) 93–102.
[27] Y. Duan, X. Guan, J. Ge, D. Quan, Y. Zhuo, H. Ye, T. Shao, Cationic nano-copolymers mediated IKKbeta targeting siRNA inhibit the proliferation of human Tenon's capsule fibroblasts in vitro, Mol. Vis. 14 (2008) 2616–2628.
[28] J. Molpeceres, M. Guzman, M.R. Aberturas, M. Chacon, L. Berges, Application of central composite designs to the preparation of polycaprolactone nanoparticles by solvent displacement, J. Pharm. Sci. 85 (1996) 206–213.
[29] A. Diaz-Moscoso, D. Vercauteren, J. Rejman, J.M. Benito, C. Ortiz Mellet, S.C. De Smedt, J.M. Fernandez, Insights in cellular uptake mechanisms of pDNA-polycationic amphiphilic cyclodextrin nanoparticles (CDplexes), J. Control. Release 143 (2010) 318–325.

[30] O.M. Merkel, M. Zheng, M.A. Mintzer, G.M. Pavan, D. Librizzi, M. Maly, H. Hoffken, A. Danani, E.E. Simanek, T. Kissel, Molecular modeling and in vivo imaging can identify successful flexible triazine dendrimer-based siRNA delivery systems, J. Control. Release (2011), doi:10.1016/j.jconrel.2011.1002.1016.
[31] D.S. Friend, D. Papahadjopoulos, R.J. Debs, Endocytosis and intracellular processing accompanying transfection mediated by cationic liposomes, Biochim. Biophys. Acta 1278 (1996) 41–50.
[32] T. Merdan, K. Kunath, D. Fischer, J. Kopecek, T. Kissel, Intracellular processing of poly(ethylene imine)/ribozyme complexes can be observed in living cells by using confocal laser scanning microscopy and inhibitor experiments, Pharm. Res. 19 (2002) 140–146.
[33] S. Zhu, M. Hong, L. Zhang, G. Tang, Y. Jiang, Y. Pei, PEGylated PAMAM dendrimer–doxorubicin conjugates: in vitro evaluation and in vivo tumor accumulation, Pharm. Res. 27 (2010) 161–174.
[34] J. Contreras, J. Xie, Y.J. Chen, H. Pei, G. Zhang, C.L. Fraser, S.F. Hamm-Alvarez, Intracellular uptake and trafficking of difluoroboron dibenzoylmethane-polylactide nanoparticles in HeLa cells, ACS Nano 4 (2010) 2735–2747.
[35] K.L. Douglas, C.A. Piccirillo, M. Tabrizian, Cell line-dependent internalization pathways and intracellular trafficking determine transfection efficiency of nanoparticle vectors, Eur. J. Pharm. Biopharm. 68 (2008) 676–687.
[36] J. Panyam, W.Z. Zhou, S. Prabha, S.K. Sahoo, V. Labhasetwar, Rapid endo-lysosomal escape of poly(DL-lactide-co-glycolide) nanoparticles: implications for drug and gene delivery, Faseb J. 16 (2002) 1217–1226.
[37] T.E. Tjelle, A. Brech, L.K. Juvet, G. Griffiths, T. Berg, Isolation characterization of early endosomes late endosomes and terminal lysosomes: their role in protein degradation, J. Cell Sci. 109 (Pt 12) (1996) 2905–2914.
[38] L.H. Wang, K.G. Rothberg, R.G. Anderson, Mis-assembly of clathrin lattices on endosomes reveals a regulatory switch for coated pit formation, J. Cell Biol. 123 (1993) 1107–1117.
[39] J.E. Heuser, R.G. Anderson, Hypertonic media inhibit receptor-mediated endocytosis by blocking clathrin-coated pit formation, J. Cell Biol. 108 (1989) 389–400.
[40] J.E. Schnitzer, P. Oh, E. Pinney, J. Allard, Filipin-sensitive caveolae-mediated transport in endothelium: reduced transcytosis scavenger endocytosis and capillary permeability of select macromolecules, J. Cell Biol. 127 (1994) 1217–1232.
[41] K.G. Rothberg, J.E. Heuser, W.C. Donzell, Y.S. Ying, J.R. Glenney, R.G. Anderson, Caveolin a protein component of caveolae membrane coats, Cell 68 (1992) 673–682.
[42] N. Araki, M.T. Johnson, J.A. Swanson, A role for phosphoinositide 3-kinase in the completion of macropinocytosis and phagocytosis by macrophages, J. Cell Biol. 135 (1996) 1249–1260.
[43] E.P. Kilsdonk, P.G. Yancey, G.W. Stoudt, F.W. Bangerter, W.J. Johnson, M.C. Phillips, G.H. Rothblat, Cellular cholesterol efflux mediated by cyclodextrins, J. Biol. Chem. 270 (1995) 17250–17256.
[44] S.K. Rodal, G. Skretting, O. Garred, F. Vilhardt, B. van Deurs, K. Sandvig, Extraction of cholesterol with methyl-beta-cyclodextrin perturbs formation of clathrin-coated endocytic vesicles, Mol. Biol. Cell 10 (1999) 961–974.
[45] J. Rejman, A. Bragonzi, M. Conese, Role of clathrin- and caveolae-mediated endocytosis in gene transfer mediated by lipo- and polyplexes, Mol. Ther. 12 (2005) 468–474.
[46] S.M. Moghimi, P. Symonds, J.C. Murray, A.C. Hunter, G. Debska, A. Szewczyk, A two-stage poly(ethylenimine)-mediated cytotoxicity: implications for gene transfer/therapy, Mol. Ther. 11 (2005) 990–995.
[47] F.J. Martin, R.C. MacDonald, Lipid vesicle-cell interactions. III. Introduction of a new antigenic determinant into erythrocyte membranes, J. Cell Biol. 70 (1976) 515–526.
[48] G. Poste, D. Papahadjopoulos, Lipid vesicles as carriers for introducing materials into cultured cells: influence of vesicle lipid composition on mechanism(s) of vesicle incorporation into cells, Proc. Natl. Acad. Sci. USA 73 (1976) 1603–1607.
[49] I.S. Zuhorn, U. Bakowsky, E. Polushkin, W.H. Visser, M.C. Stuart, J.B. Engberts, D. Hoekstra, Nonbilayer phase of lipoplex-membrane mixture determines endosomal escape of genetic cargo and transfection efficiency, Mol. Ther. 11 (2005) 801–810.